Physics Letters B 802 (2020) 135215

Contents lists available at ScienceDirect

Physics Letters B

www.elsevier.com/locate/physletb

Restoration of the natural $E(1/2_1^+)$ - $E(3/2_1^+)$ energy splitting in odd-K isotopes towards N = 40

Y.L. Sun [a,b,*], A. Obertelli [a,b,c], P. Doornenbal [c], C. Barbieri [d], Y. Chazono [e], T. Duguet [b,f], H.N. Liu [a,b,g], P. Navrátil [h], F. Nowacki [i,j], K. Ogata [e,k], T. Otsuka [l,m], F. Raimondi [d,n], V. Somà [b], Y. Utsuno [o], K. Yoshida [o], N. Achouri [p], H. Baba [c], F. Browne [c], D. Calvet [b], F. Château [b], S. Chen [q,c,r], N. Chiga [c], A. Corsi [b], M.L. Cortés [c], A. Delbart [b], J.-M. Gheller [b], A. Giganon [b], A. Gillibert [b], C. Hilaire [b], T. Isobe [c], T. Kobayashi [s], Y. Kubota [c,m], V. Lapoux [b], T. Motobayashi [c], I. Murray [c], H. Otsu [c], V. Panin [c], N. Paul [b], W. Rodriguez [t,c], H. Sakurai [c,l], M. Sasano [c], D. Steppenbeck [c], L. Stuhl [m], Y. Togano [u], T. Uesaka [c], K. Wimmer [l], K. Yoneda [c], O. Aktas [g], T. Aumann [a,v], L.X. Chung [w], F. Flavigny [p], S. Franchoo [p], I. Gašparić [x,c], R.-B. Gerst [y], J. Gibelin [z], K.I. Hahn [aa], D. Kim [aa,c], T. Koiwai [l], Y. Kondo [ab], P. Koseoglou [a,v], J. Lee [r], C. Lehr [a], B.D. Linh [w], T. Lokotko [r], M. MacCormick [p], K. Moschner [y], T. Nakamura [ab], S.Y. Park [aa,c], D. Rossi [a], E. Sahin [ac], D. Sohler [ad], P.-A. Söderström [a], S. Takeuchi [ab], H. Törnqvist [a,v], V. Vaquero [ae], V. Wagner [a], S. Wang [af], V. Werner [a], X. Xu [r], H. Yamada [ab], D. Yan [af], Z. Yang [c], M. Yasuda [ab], L. Zanetti [a]

[a] Institut für Kernphysik, Technische Universität Darmstadt, D-64289 Darmstadt, Germany
[b] IRFU, CEA, Université Paris-Saclay, F-91191 Gif-sur-Yvette, France
[c] RIKEN Nishina Center, 2-1 Hirosawa, Wako, Saitama 351-0198, Japan
[d] Department of Physics, University of Surrey, Guildford GU2 7XH, UK
[e] Research Center for Nuclear Physics (RCNP), Osaka University, Ibaraki 567-0047, Japan
[f] KU Leuven, Instituut voor Kern- en Stralingsfysica, 3001 Leuven, Belgium
[g] Department of Physics, Royal Institute of Technology, SE-10691 Stockholm, Sweden
[h] TRIUMF, 4004 Wesbrook Mall, Vancouver, British Columbia V6T 2A3, Canada
[i] Université de Strasbourg, IPHC, 67037 Strasbourg Cedex, France
[j] CNRS, UMR7178, 67037 Strasbourg, France
[k] Department of Physics, Osaka City University, Osaka 558-8585, Japan
[l] Department of Physics, University of Tokyo, 7-3-1 Hongo, Bunkyo, Tokyo 113-0033, Japan
[m] Center for Nuclear Study, University of Tokyo, RIKEN campus, Wako, Saitama 351-0198, Japan
[n] ESNT, CEA, Université Paris-Saclay, F-91191 Gif-sur-Yvette, France
[o] Japan Atomic Energy Agency, Tokai, Ibaraki 319-1195, Japan
[p] Institut de Physique Nucléaire, CNRS-IN2P3, Université Paris-Sud, Université Paris-Saclay, 91406 Orsay Cedex, France
[q] State Key Laboratory of Nuclear Physics and Technology, Peking University, Beijing 100871, PR China
[r] Department of Physics, The University of Hong Kong, Pokfulam, Hong Kong
[s] Department of Physics, Tohoku University, Sendai 980-8578, Japan
[t] Universidad Nacional de Colombia, Sede Bogota, Facultad de Ciencias, Departamento de Física, Bogotá 111321, Colombia
[u] Department of Physics, Rikkyo University, 3-34-1 Nishi-Ikebukuro, Toshima, Tokyo 172-8501, Japan
[v] GSI Helmoltzzentrum für Schwerionenforschung GmbH, Planckstr. 1, 64291 Darmstadt, Germany
[w] Institute for Nuclear Science & Technology, VINATOM, P.O. Box 5T-160, Nghia Do, Hanoi, Viet Nam
[x] Ruđer Bošković Institute, Bijenička cesta 54, 10000 Zagreb, Croatia
[y] Institut für Kernphysik, Universität zu Köln, D-50937 Cologne, Germany
[z] LPC Caen, ENSICAEN, Université de Caen, CNRS/IN2P3, F-14050 Caen, France
[aa] Department of Science Education and Department of Physics, Ewha Womans University, Seoul 03760, Republic of Korea
[ab] Department of Physics, Tokyo Institute of Technology, 2-12-1 O-Okayama, Meguro, Tokyo, 152-8551, Japan
[ac] Department of Physics, University of Oslo, N-0316 Oslo, Norway
[ad] MTA Atomki, P.O. Box 51, Debrecen H-4001, Hungary
[ae] Instituto de Estructura de la Materia, CSIC, E-28006 Madrid, Spain
[af] Institute of Modern Physics, Chinese Academy of Sciences, Lanzhou, PR China

* Corresponding author at: Institut für Kernphysik, Technische Universität Darmstadt, D-64289 Darmstadt, Germany.
E-mail address: ysun@ikp.tu-darmstadt.de (Y.L. Sun).

https://doi.org/10.1016/j.physletb.2020.135215

ARTICLE INFO

Article history:
Received 9 September 2019
Received in revised form 26 December 2019
Accepted 10 January 2020
Available online 16 January 2020
Editor: D.F. Geesaman

Keywords:
Spectroscopy
Shell evolution
^{51}K
^{53}K

ABSTRACT

We report on the first γ-ray spectroscopy of ^{51,53}K produced via the ^{52,54}Ca(p,2p) reactions at ~250 MeV/nucleon. Unambiguous final-state angular-momentum assignments were achieved for beam intensities down to few particles per second by using a new technique based on reaction vertex tracking combined with a thick liquid-hydrogen target. Through γ-ray spectroscopy and exclusive parallel momentum distribution analysis, $3/2^+$ ground states and $1/2^+$ first excited states in ^{51,53}K were established quantifying the natural ordering of the $1d_{3/2}$ and $2s_{1/2}$ proton-hole states that are restored at N = 32 and 34. State-of-the-art *ab initio* calculations and shell-model calculations with improved phenomenological effective interactions reproduce the present data and predict consistently the increase of the $E(1/2_1^+)$ - $E(3/2_1^+)$ energy differences towards N = 40.

The atomic nucleus is a strongly interacting many-body system that, however, shows features of independent nucleon motion near the Fermi surface [1]. The first predictive realization of the independent-particle model was achieved by Mayer and Jensen [2,3], who established the conventional nuclear shell structure by introducing a strong spin-orbit coupling to explain the "magic numbers" and the ground-state spins of stable odd-mass-number nuclei. In the modern shell-model approach, the variation of the nuclear structure is mainly driven by the monopole component of the interaction, which is responsible for the single-particle behavior, and further modified by multiple correlations [4,5]. The correlation effects vanish in nuclei with a one-particle or one-hole configuration with respect to closed shells, resulting in the so-called monopole energy shift along the corresponding isotopic or isotonic chains [6,7]. In this situation the single-particle energies of the odd nucleon are solely determined by the monopole interaction and change as linear functions of the nucleon number of the other type.

Recently, significant experimental and theoretical efforts have focused on the monopole shift of proton-hole states in the neutron-rich odd-K isotopes [8–14], where Z = 20 remains a shell closure away from stability [15,16]. From ^{39}K (N = 20) to ^{47}K (N = 28), the energy level splitting between the $1/2_1^+$ and $3/2_1^+$ states drops rapidly and the $1/2_1^+$ state becomes lower in energy than the $3/2_1^+$ state in ^{47}K [17–19], which is interpreted as an energy inversion of the $\pi 1d_{3/2}$ and $\pi 2s_{1/2}$ orbitals at N = 28 [9–11,18]. The energy splitting decreases almost in proportion to the number of valence neutrons in the $f_{7/2}$ orbital, reflecting the robust feature of the monopole interaction [20]. For K isotopes beyond N = 28 where the valence neutrons start filling the $p_{3/2}$ and $p_{1/2}$ orbitals, data are scarce. The only known energy splitting is for ^{49}K (N = 30), in which the $1/2^+$ ground state and the $3/2_1^+$ excited state become nearly degenerate [13,21]. Predictions from phenomenological shell-model calculations using different effective interactions reproduce well the energy splittings from ^{39}K to ^{49}K but differ significantly at N = 32 and 34 [14]. A ground-state spin I = 3/2 has been recently established in ^{51}K [13] using laser spectroscopy, indicating that the $\pi 1d_{3/2}$ and $\pi 2s_{1/2}$ orbitals restore natural order at N = 32. However, the energy splitting in ^{51}K was still unknown, since the $1/2_1^+$ excitation energy in ^{51}K has not been measured. For ^{53}K and beyond, no spectroscopic information was known. The measurements towards ^{59}K (N = 40) are essential to understand the development of collectivity towards the potentially doubly magic nucleus ^{60}Ca discovered newly [22]. More recently, the proton structure of K and Ca isotopes beyond N = 28 has attracted particular interest with a steep raise of charge radii up to ^{51}K [23] and ^{52}Ca [24], which can be understood as due to the halo-like nature of the $\nu 2p_{3/2}$ orbital [25]. In this Letter, we report on the first measurement of low-lying states in ^{51,53}K populated by one-proton removal from doubly magic nuclei ^{52,54}Ca and the unambiguous angular-momentum assignments of the populated $1/2_1^+$ and $3/2_1^+$ states.

The experiment was performed at the Radioactive Isotope Beam Factory operated by the RIKEN Nishina Center and the Center for Nuclear Study of the University of Tokyo. The radioactive isotopes were produced by fragmentation of a 345 MeV/nucleon ^{70}Zn primary beam on a Be target with an average beam intensity of 240 pnA. The secondary cocktail beam was identified using the magnetic rigidity ($B\rho$), energy loss (ΔE) and time-of-flight (TOF) information in the BigRIPS two-stage fragment separator [26,27]. The mean intensities of the ^{52}Ca and ^{54}Ca secondary beams were 4.4 and 7.3 particles per second, respectively.

The ^{52}Ca and ^{54}Ca secondary beams with average kinetic energies of 266 and 251 MeV/nucleon, respectively, impinged on a 151(1)-mm-thick liquid hydrogen (LH_2) target [30] to induce one-proton knockout reactions. The incident angle and position of the projectiles were determined by two multi-wire drift chambers (MWDCs). The heavy fragments were measured by the SAMURAI spectrometer [31] with a central magnetic field of 2.7 Tesla. Trajectories of the charged fragments were determined by two MWDCs located at the entrance and exit of the SAMURAI magnet. The ΔE and TOF of the fragments were measured by a 24-element 10-mm-thick plastic scintillator hodoscope. ^{51,53}K from the ^{52,54}Ca(p,2p) reactions could be clearly identified using the $B\rho$-ΔE-TOF method [32] and were fully within the acceptance of the spectrometer.

The LH_2 target was surrounded by the MINOS time projection chamber [33] to track the outgoing protons for reaction vertex reconstruction. The estimated vertex resolution was ~4 mm (FWHM) [34]. Velocities of the projectiles and residues at the reaction vertex were deduced by taking into account the energy loss in the materials along their trajectories. The efficiencies of detecting at least one proton for ^{52}Ca(p,2p)^{51}K and ^{54}Ca(p,2p)^{53}K reactions were determined to be 90(6)% and 88(5)%, respectively.

De-excitation γ-rays from the reaction residues were measured by the upgraded DALI2+ array [32,35], which consisted of 226 NaI(Tl) detectors with an average threshold set to around 50 keV. The gain of the NaI(Tl) detectors was set to measure γ-rays with energies up to ~6 MeV after Doppler correction. The whole array was calibrated with ^{60}Co, ^{137}Cs, ^{88}Y, and ^{133}Ba sources, yielding a calibration uncertainty of 4 keV. The measured energy resolution for the 662 keV γ-ray peak of ^{137}Cs was 9.1% (FWHM). To increase the full energy peak efficiency, add-back analysis was adopted for γ-ray hits in detectors located within 12 cm of each other. For 1-MeV γ-rays emitted from nuclei with a velocity of 0.6c, the simulated photopeak efficiency and energy resolution were 30% and 11% (FWHM), respectively. The Doppler-corrected γ-ray spectra of ^{51}K(^{53}K) from one-proton removal of ^{52}Ca(^{54}Ca) are displayed in

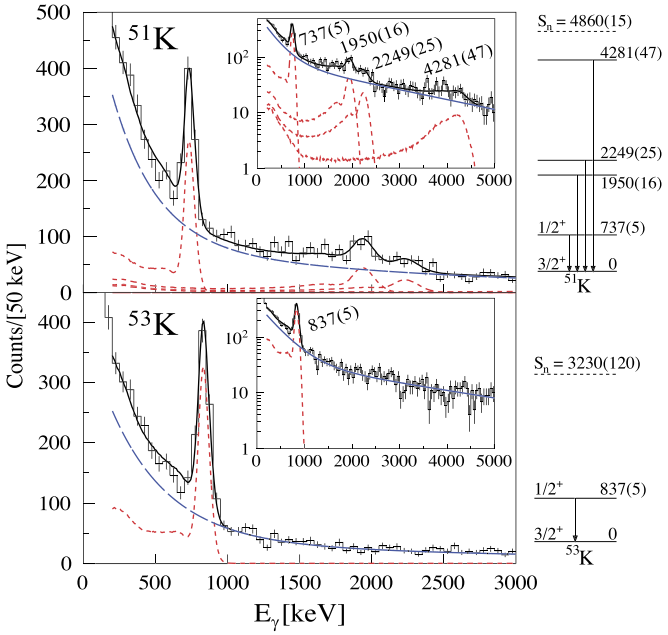

Fig. 1. Doppler-corrected γ-ray spectra of ^{51}K (upper panel) and ^{53}K (lower panel). The black solid lines show the fit results of the simulated response functions for the observed transitions (red dotted lines) and double exponential backgrounds (blue dashed lines). The insets show the spectra up to 5 MeV. The deduced experimental level schemes are shown to the right of the spectra. The experimental neutron separation energies (S_n) are taken from Refs. [28,29].

Fig. 1. The spectra were fitted with GEANT4 [36] simulated response functions on top of a double-exponential background to determine the transition energies and intensities. For ^{51}K, three transitions at 737(5), 1950(16), 2249(25) keV were clearly observed and one structure at 4281(47) keV was observed with a significance level of 3.0 standard deviations (σ). In the case of ^{53}K, only one clear γ-ray transition at 837(5) keV was observed. All the transitions were attributed to direct decays to the ground states as no γ-γ coincidences were observed. In this work, we focus on the first two low-lying states in ^{51,53}K, whose extracted cross sections are listed in Table 1. The quoted uncertainties for the excited states include contributions from statistics, MINOS efficiency (7%) and γ-ray detection efficiency (5%). The reaction losses of ^{52,54}Ca and ^{51,53}K in the materials along their trajectories were determined by measuring the corresponding unreacted beam and were taken into account in the cross-section deduction. The measured inclusive cross sections of ^{52}Ca(p,2p)^{51}K and ^{54}Ca(p,2p)^{53}K reactions were 9.0(6) mb and 5.3(3) mb, respectively. Only one gamma-ray transition was observed in ^{53}K. While three other transitions were observed in ^{51}K in addition to the transition from its first excited state, amounting to a cross section of 2.1(3) mb to the corresponding excited states. The ground-state population cross sections were deduced after subtracting the excited-state contributions from the inclusive yields assuming that there are no higher excited states decaying by emitting γ-rays beyond 5 MeV, since the neutron separation energies of ^{51}K(^{53}K) is 4.86 MeV [28] (3.23 MeV [29]).

The measured partial cross sections are compared to the products of the single-particle cross sections (σ_{sp}) obtained using the distorted-wave impulse-approximation (DWIA) model of Refs. [37,38] and the spectroscopic factors (SFs) obtained using either the self-consistent Green's function (SCGF) approach in the third-order algebraic diagrammatic construction [ADC(3)] approximation [39] with the chiral interaction NN+3N(lnl) [40] or large-scale shell-model (LSSM) calculations with phenomenological effective interactions discussed later in the text. The DWIA model has been applied to calculate σ_{sp} for (p,2p) reactions in recent works [41–43]. Here, the proton single-particle wave functions were determined by a mean-field Hartree-Fock-Bogoliubov approach with the SLy4 interaction [44]. The energy dependence of the cross sections was considered by taking the σ_{sp} averaged over the beam energy along the thick target. The SCGF SFs are systematically smaller than the shell-model SFs because of the particle-vibration coupling effects that cannot be accounted even in LSSM valence spaces [45]. As shown in Table 1, the experimental cross sections to the ground states are 3.1(4) and 2.5(4) times of the cross sections to the first excited states for ^{51}K and ^{53}K, respectively, while the theoretical ratios of these two states are around 2.0 due to the fact that theoretical calculations overestimate the cross sections for the $1/2^+_1$ states. Nevertheless, the experimental ground-state population cross sections are higher than those of the first excited states, consistent with the removal of proton in $1d_{3/2}$ and $2s_{1/2}$ orbitals with occupancy of $2j$+1 = 4 and 2, respectively. In addition to this first indication, the spin-parity assignments are determined unambiguously using the parallel momentum distribution (PMD) of the residual nuclei, which links its shape directly to the orbital angular momentum of the knocked-out proton [46].

Fig. 2 displays the PMDs of ^{51,53}K from the ^{52,54}Ca(p,2p) reactions which were obtained by transforming the measured momentum of the residues to the beam-at-rest frame to eliminate the momentum spread of the incident beam. Parallel momentum resolutions of σ = 37 MeV/c and 43 MeV/c were achieved for the ^{52}Ca(p,2p)^{51}K and ^{54}Ca(p,2p)^{53}K reactions, respectively, by taking into account the measured momentum resolution using the unreacted beam and the momentum spread due to the vertex resolution. The angular-momentum assignments were determined by comparing the measured PMDs to DWIA predictions [37] assuming removal of the proton from different single-particle orbitals and folded with the experimental momentum resolutions. The PMDs of the 737-keV state in ^{51}K and the 837-keV state in ^{53}K can be well reproduced by the theoretical curves assuming removal of an s-wave proton from ^{52}Ca and ^{54}Ca, respectively. The assignments are strongly supported by the $\log_{10}$ scaled Bayes factors [47] of s-wave over d-wave which are 3 and 7 for ^{51}K and ^{53}K, respec-

Table 1
The measured excitation energies (E_{exp}), spin-parity (J^π) and cross sections (σ_{exp}) from the ^{52,54}Ca(p,2p)^{51,53}K reactions. Only the $1/2^+_1$ and $3/2^+_1$ states are listed. Theoretical excitation energies (E_{th}), J^π, and spectroscopic factors (SF_{th}) are obtained from *ab initio* SCGF calculations with the NN+3N(lnl) interaction (Th.1) or shell-model calculations with the SDPF-Umod interaction (Th.2) or the SDPF-MUs interaction (Th.3). Theoretical partial cross sections (σ_{th}) are the products of the SF_{th} and the single-particle cross sections (σ_{sp}) calculated using the DWIA model. See text for details.

	E_{exp} (keV)	J^π	σ_{exp} (mb)	E_{th} (keV)			J^π	SF_{th}			σ_{sp} (mb)	σ_{th} (mb)		
				Th.1	Th.2	Th.3		Th.1	Th.2	Th.3		Th.1	Th.2	Th.3
^{51}K	0	$3/2^+$	5.2(4)	0	0	0	$3/2^+$	2.76	3.65	3.53	1.73	4.77	6.31	6.11
	737(5)	$1/2^+$	1.7(2)	883	747	846	$1/2^+$	1.27	1.68	1.59	1.88	2.39	3.16	2.99
^{53}K	0	$3/2^+$	3.8(3)	0	0	0	$3/2^+$	2.90	3.80	3.71	1.49	4.32	5.66	5.53
	837(5)	$1/2^+$	1.5(2)	717	560	794	$1/2^+$	1.36	1.74	1.66	1.64	2.23	2.85	2.72

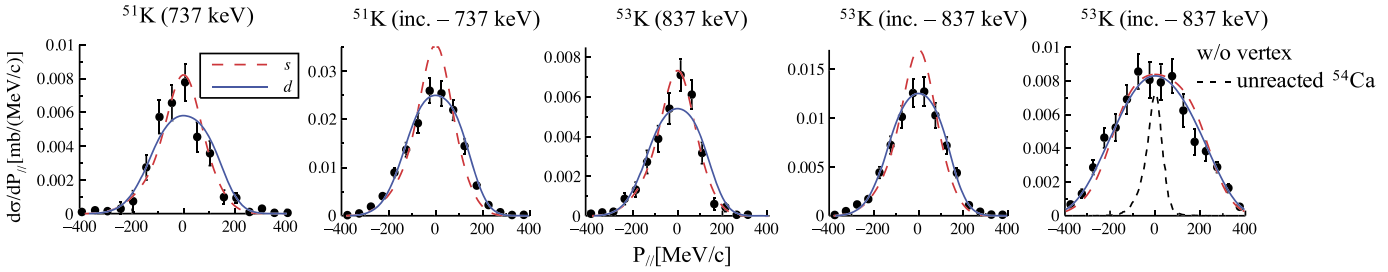

Fig. 2. Individual parallel momentum distributions of the ^{51,53}K residues from the ^{52,54}Ca(p,2p) reactions compared to the DWIA calculated momentum distributions assuming removal of a $2s_{1/2}$ or $1d_{3/2}$ proton. Theoretical curves have been convoluted with the experimental resolutions and normalized to the experimental cross sections. The right most panel shows the momentum distribution of ^{53}K without vertex and the momentum distribution from unreacted ^{54}Ca beam.

tively. [1] Thereby, the spins and parities of the first excited states of ^{51,53}K are assigned as $1/2^+$. To pin down the angular momenta of the ground states, we subtracted the first-excited-state PMDs from the inclusive spectra. The resulting distributions are dominated by the ground-state contribution (71% in ^{51}K and 100% in ^{53}K), and can be well reproduced by the DWIA calculation assuming removal of d-wave protons. For the ground states the $\log_{10}$ scaled Bayes factors of d-wave over s-wave are 100 and 77 for ^{51}K and ^{53}K, respectively. Spins and parities of $3/2^+$ are therefore established for the ground states of ^{51,53}K. No bound fp-shell states in ^{51,53}K could be populated via (p,2p) reactions based on the *ab initio* SCGF calculations, which is in line with the doubly magic nature of ^{52,54}Ca. Note that the momentum resolution without using the vertex information would not be sufficient to disentangle the s- and d-wave contributions as illustrated in the rightmost panel of Fig. 2. This is the first time the PMDs are extracted with enough resolving power to disentangle proton removal from different ℓ orbitals when using thick targets, pushing the sensitivity frontiers for the spectroscopy of very exotic nuclei produced at only few particles per second.

We now discuss the $E(1/2^+_1)$ - $E(3/2^+_1)$ systematics in odd-K isotopes. As displayed in Fig. 3, the reinversion of the $3/2^+_1$ and $1/2^+_1$ proton-hole states in ^{51}K is confirmed and its continuation to ^{53}K is established for the first time. We compare the experimental energy splittings to $0\hbar\omega$ LSSM calculations performed in the *sd-pf* valence space employing the SDPF-U interaction [9] and effective interactions based on the SDPF-MU Hamiltonian [11]. The shell-model calculations show excellent agreement with the experimental results from ^{39}K to ^{49}K and start to differ significantly at ^{51}K. The SDPF-U calculation underestimates the energy splitting by ∼0.3 MeV in ^{51}K and by ∼0.7 MeV in ^{53}K. To improve the SDPF-U interaction in the N > 30 region, the $\pi 1d_{3/2}$-$\nu 2p_{3/2}p_{1/2}$ and $\pi 2s_{1/2}$-$\nu 2p_{3/2}p_{1/2}$ monopoles need to be tuned by +37.5 keV and -75 keV, respectively, leading to the SDPF-Umod interaction. The predicted energy splittings in ^{51,53}K using the SDPF-Umod interaction are much closer to the data, increasing by 277 keV and 410 keV, respectively, demonstrating a strong sensitivity to these specific proton-neutron cross-shell interactions. Note that the modified SDPF-U interaction can well reproduce the measured 2^+_1 systematics in Ca isotopes and the single particle spectra in N = 21 isotones [9]. Regarding the SDPF-MU Hamiltonian [11], it has been successfully applied to the present mass region. It was derived based on the $V_{\rm MU}$ interaction which is suitable for a global description as its six parameters of Gaussian central force were determined from G-matrix and effective interactions in the *sd*- and *pf*-shells [48]. The SDPF-MUr [49] is a revision made for ^{49}K [13, 21] and ^{54}Ca [16]. ^{51,53}K provide a precious opportunity to further tune certain two-body matrix elements beyond the global determination. In order to describe the measured energy splittings, a modification is required to shift the original T = 0 central force monopole strength between $\pi 2s_{1/2}$ and $\nu 2p_{1/2}$ (-1.27 MeV) and between $\pi 2s_{1/2}$ and $\nu 2p_{3/2}$ (-1.29 MeV) by -0.2 MeV, meaning strengthening the attraction. In addition, the $\nu 1f^2_{5/2}$ pairing matrix element is shifted by -0.4 MeV to better describe the 2^+ in Ca isotopes, which has no direct relevance to the present case. The derived SDPF-MUs interaction with the above modifications can reproduce the observed splittings from ^{39}K to ^{53}K. The original SDPF-MU interaction produces the T = 0 monopole strength between $\pi 2s_{1/2}$ and $\nu 2p_{1/2}$ and that between $\pi 2s_{1/2}$ and $\nu 2p_{3/2}$, both larger in magnitude compared to other cases because that the relative wave functions contains more components with lower relative orbital angular momentum, such as the relative s-wave, and the employed Gaussian central force produces a flat contribution at short distances [48]. This short-range behavior of the effective *NN* interaction does not show up in most other monopole strengths. Such information is a unique outcome of the present experiment and will be very useful in obtaining more insight of the effective *NN* interaction, including global ones like SDPF-MU's. Note that the above-discussed modifications of interactions have negligible impact on the total binding energy, which in the shell-model approach involves all monopole interactions and depends on the sum

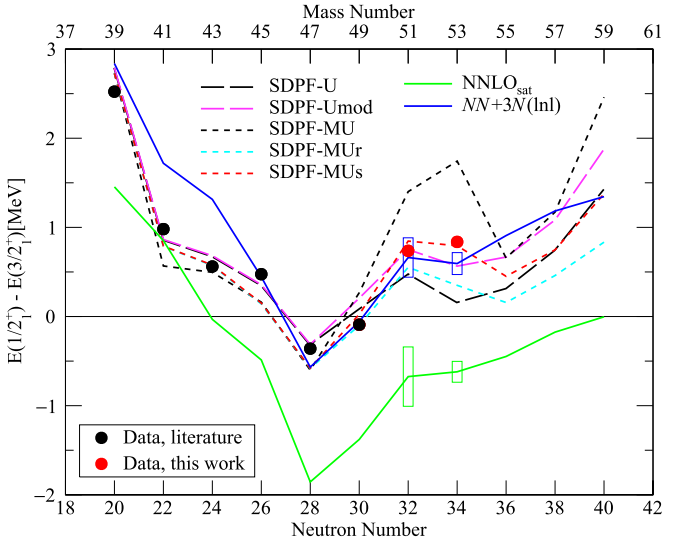

Fig. 3. Energy splitting between the $1/2^+_1$ and $3/2^+_1$ states in the odd-K isotopes compared to shell-model calculations using the SDPF-U [9], the SDPF-Umod, the SDPF-MU [11], the SDPF-MUr [49], the SDPF-MUs effective interactions and the *ab initio* SCGF calculation employing the NNLO$_{\rm sat}$ [54] and the *NN*+3*N*(lnl) [40] interactions. The rectangular regions for ^{51,53}K represent estimated theoretical uncertainties due to many-body truncations. Experimental data are taken from Ref. [21] and this work.

[1] One hypothesis has decisive evidence against the other one if their $\log_{10}$ scaled Bayes factor is larger than 2.

of their absolute values, as illustrated in the parameterization of the Duflo-Zuker shell-model mass formula [50,51].

In the shell-model calculations, the increased energy splitting from ^{49}K to ^{51,53}K is a consequence of the restoration of a sizeable Z = 16 sub-shell gap in ^{51}K and ^{53}K, which are calculated to be 0.95 MeV and 1.38 MeV, respectively, when the SDPF-MUs interaction is employed. The near degeneracy of the $\pi 1d_{3/2}$ and $\pi 2s_{1/2}$ orbitals around N = 28 has been suggested to play a key role in the development of collectivity in neutron-rich silicon, sulfur and argon isotopes [11,52,53]. The restoration of the Z = 16 sub-shell gap would therefore have the profound consequence of suppressing the collectivity induced by proton excitations for Z = 14, 16, 18 nuclei lying beyond N = 30. Indeed, a narrowed shell gap will free nucleons to participate in collective motions, while a large shell gap will quench correlations by enlarging the energy cost for excitations across the gaps.

The energy splittings along the odd-K isotopic chain also provide a testing ground to validate the chiral effective field theory (EFT) interactions in the *ab initio* many-body calculations, which have extended their reach to entire medium-mass isotopic chains very recently. In particular, we compare the experimental data to the initial ADC(2) Gorkov-SCGF calculations [55,56] performed in a model space of up to 14 harmonic oscillator shells including three-nucleon (3N) interactions limited to basis states with $N_1 + N_2 + N_3 \leq 16$ where $N = 2n + l$. We employed two sets of state-of-the-art EFT interactions: the NNLO$_{\rm sat}$ [54] and the newly developed NN+3N(lnl) [40]. Uncertainties associated with the approximated many-body scheme were estimated by differences between ADC(2) and available ADC(3) results. With the most recent NN+3N(lnl) interaction, SCGF total binding energies in this mass region are within 3% (1%) from experiment when computed in the ADC(2) [ADC(3)] scheme [57]. As shown in Fig. 3, the NNLO$_{\rm sat}$ calculations systematically underestimate the splittings in odd-K isotopes by $\sim$1 MeV, although the same interaction successfully reproduces charge radii, binding energies and spectroscopic properties of lighter medium-mass nuclei [54,58]. In contrast, the NN+3N(lnl) calculations show better overall agreement with the experimental data, consistent with its application on the mass prediction of $^{48-56}$Ti [40].

So far, state-of-the-art shell-model and *ab initio* calculations reproduce experimental energy splittings at all the shell closures including N = 20, 28, 32, 34. The *ab initio* NN+3N(lnl) calculations predict that the energy splitting increases linearly from 0.59 MeV in ^{53}K to 1.35 MeV in ^{59}K. The two modified phenomenological effective interactions SDPF-Umod and SDPF-MUs anticipate similar trends as shown in Fig. 3, reaching 1.88 MeV and 1.38 MeV at ^{59}K, respectively, equivalent to the corresponding effective single-particle energy differences between the $\pi 1d_{3/2}$ and $\pi 2s_{1/2}$ orbitals. Since the valence neutrons in the shell-model calculations are restricted to *pf*-shells below N = 40, the consistent energy-splitting increase towards ^{59}K, still to be proven experimentally, supports the N = 40 shell closure assumed in all the above shell-model calculations.

In summary, we have reported on the first measurement of the low-lying states in ^{51,53}K populated from the ^{52,54}Ca(p,2p) reactions at $\sim$250 MeV/nucleon. We implemented a new technique based on reaction vertex tracking to achieve momentum resolutions of $\sim$40 MeV/c when using a thick liquid-hydrogen target. The $1/2^+_1 \rightarrow 3/2^+_1$ transitions of ^{51,53}K were measured for the first time and the spins-parities were unambiguously assigned based on the measured cross sections and parallel momentum distributions. The measured $E(1/2^+_1)$ - $E(3/2^+_1)$ energy splittings in ^{51,53}K provide a stringent constraint on the $\pi 2s_{1/2}1d_{3/2}$-$\nu 2p_{1/2}p_{3/2}$ matrix elements. The restoration of the natural ordering of the $1/2^+_1$ and $3/2^+_1$ proton-hole states in ^{51,53}K is interpreted as a restoration of a sizeable Z = 16 sub-shell gap beyond N = 30, having as a consequence the suppression of proton-induced collectivity in the region. State-of-the-art shell model calculations and *ab initio* calculations all predict consistently the continuation and enhancement of the restoration towards N = 40.

Acknowledgements

We are very grateful to the RIKEN Nishina Center accelerator staff for providing the stable and high-intensity zinc beam and to the BigRIPS team for the smooth operation of the secondary beams. The development of MINOS has been supported by the European Research Council through the ERC Grant No. MINOS-258567. Green's function calculations were performed using HPC resources from GENCI-TGCC, France (Projects A0030507392 and A0050507392) and from the DiRAC Data Intensive service at Leicester, UK (funded by the UK BEIS via STFC capital grants ST/K000373/1 and ST/R002363/1 and STFC DiRAC Operations grant ST/R001014/1). This work (C. B.) was also supported by the United Kingdom Science and Technology Facilities Council (STFC) under Grants No. ST/P005314/1 and No. ST/L005816/1. K. O. acknowledges the support by Grant-in-Aid for Scientific Research JP16K05352. Y. L. S. acknowledges the support of Marie Skłodowska-Curie Individual Fellowship (H2020-MSCA-IF-2015-705023) from the European Union and the support from the Helmholtz International Center for FAIR. The valuable discussions with C. Qi are gratefully acknowledged. H. N. L. acknowledges the support from the Enhanced Eurotalents program (PCOFUND-GA-2013-600382) co-funded by CEA and the European Union. H. N. L. and A. O. acknowledge the support from the Deutsche Forschungsgemeinschaft (DFG, German Research Foundation) - Project No. 279384907-SFB 1245. Y. L. S. and A. O. acknowledge the support from the Alexander von Humboldt Foundation. L. X. C. and B. D. L would like to thank MOST for its support through the Physics Development Program Grant No. ĐTĐLCN.25/18. I.G. has been supported by HIC for FAIR and HRZZ under project No. 1257 and 7194. K. I. H., D. K. and S. Y. P. acknowledge the support from the NRF grant funded by the Korea government (No. 2017R1A2B2012382 and 2019M7A1A1033186). F. B. acknowledge the support from the RIKEN Special Postdoctoral Researcher Program. D.S. was supported by projects No. GINOP-2.3.3-15-2016-00034 and No. K128947. V. V. acknowledges support from the Spanish Ministerio de Economía y Competitividad under Contract No. FPA2017-84756-C4-2-P. V. W. acknowledges support from BMBF grants 05P15RDFN1, 05P19RDFN1 and DFG grant SFB 1245. P. K. acknowledges support from HGS-HIRe and BMBF grant 05P19RDFN1. This work was also supported by NKFIH (128072).

References

[1] W. Dickhoff, C. Barbieri, Self-consistent Green's function method for nuclei and nuclear matter, Prog. Part. Nucl. Phys. 52 (2) (2004) 377–496, https://doi.org/10.1016/j.ppnp.2004.02.038, http://www.sciencedirect.com/science/article/pii/S0146641004000535.

[2] M.G. Mayer, On closed shells in nuclei. II, Phys. Rev. 75 (1949) 1969–1970, https://doi.org/10.1103/PhysRev.75.1969, https://link.aps.org/doi/10.1103/PhysRev.75.1969.

[3] O. Haxel, J.H.D. Jensen, H.E. Suess, On the "magic numbers" in nuclear structure, Phys. Rev. 75 (1949) 1766, https://doi.org/10.1103/PhysRev.75.1766.2, https://link.aps.org/doi/10.1103/PhysRev.75.1766.2.

[4] E. Caurier, G. Martínez-Pinedo, F. Nowacki, A. Poves, A.P. Zuker, The shell model as a unified view of nuclear structure, Rev. Mod. Phys. 77 (2005) 427–488, https://doi.org/10.1103/RevModPhys.77.427, https://link.aps.org/doi/10.1103/RevModPhys.77.427.

[5] T. Otsuka, T. Suzuki, J.D. Holt, A. Schwenk, Y. Akaishi, Three-body forces and the limit of oxygen isotopes, Phys. Rev. Lett. 105 (2010) 032501, https://doi.org/10.1103/PhysRevLett.105.032501, https://link.aps.org/doi/10.1103/PhysRevLett.105.032501.

[6] I. Talmi, I. Unna, Order of levels in the shell model and spin of Be^{11}, Phys. Rev. Lett. 4 (1960) 469–470, https://doi.org/10.1103/PhysRevLett.4.469, https://link.aps.org/doi/10.1103/PhysRevLett.4.469.

[7] R. Bansal, J. French, Even-parity-hole states in f72-shell nuclei, Phys. Lett. 11 (2) (1964) 145–148, https://doi.org/10.1016/0031-9163(64)90648-1, http://www.sciencedirect.com/science/article/pii/0031916364906481.

[8] A. Gade, B.A. Brown, D. Bazin, C.M. Campbell, J.A. Church, D.C. Dinca, J. Enders, T. Glasmacher, M. Horoi, Z. Hu, K.W. Kemper, W.F. Mueller, T. Otsuka, L.A. Riley, B.T. Roeder, T. Suzuki, J.R. Terry, K.L. Yurkewicz, H. Zwahlen, Evolution of the $E(1/2_1^+) - E(3/2_1^+)$ energy spacing in odd-mass K, Cl, and P isotopes for $N = 20$–28, Phys. Rev. C 74 (2006) 034322, https://doi.org/10.1103/PhysRevC.74.034322, https://link.aps.org/doi/10.1103/PhysRevC.74.034322.

[9] F. Nowacki, A. Poves, Phys. Rev. C 79 (2009) 014310, https://doi.org/10.1103/PhysRevC.79.014310, https://link.aps.org/doi/10.1103/PhysRevC.79.014310.

[10] K. Kaneko, Y. Sun, T. Mizusaki, M. Hasegawa, Shell-model study for neutron-rich *sd*-shell nuclei, Phys. Rev. C 83 (2011) 014320, https://doi.org/10.1103/PhysRevC.83.014320, https://link.aps.org/doi/10.1103/PhysRevC.83.014320.

[11] Y. Utsuno, T. Otsuka, B.A. Brown, M. Honma, T. Mizusaki, N. Shimizu, Shape transitions in exotic Si and S isotopes and tensor-force-driven Jahn-Teller effect, Phys. Rev. C 86 (2012) 051301(R), https://doi.org/10.1103/PhysRevC.86.051301, https://link.aps.org/doi/10.1103/PhysRevC.86.051301.

[12] O. Sorlin, M.-G. Porquet, Evolution of the n = 28 shell closure: a test bench for nuclear forces, Phys. Scr. 2013 (T152) (2013) 014003, http://stacks.iop.org/1402-4896/2013/i=T152/a=014003.

[13] J. Papuga, M.L. Bissell, K. Kreim, K. Blaum, B.A. Brown, M. De Rydt, R.F. Garcia Ruiz, H. Heylen, M. Kowalska, R. Neugart, G. Neyens, W. Nörtershäuser, T. Otsuka, M.M. Rajabali, R. Sánchez, Y. Utsuno, D.T. Yordanov, Spins and magnetic moments of ^{49}**K** and ^{51}**K**: establishing the $1/2^+$ and $3/2^+$ level ordering beyond $n = 28$, Phys. Rev. Lett. 110 (2013) 172503, https://doi.org/10.1103/PhysRevLett.110.172503, https://link.aps.org/doi/10.1103/PhysRevLett.110.172503.

[14] J. Papuga, M.L. Bissell, K. Kreim, C. Barbieri, K. Blaum, M. De Rydt, T. Duguet, R.F. Garcia Ruiz, H. Heylen, M. Kowalska, R. Neugart, G. Neyens, W. Nörtershäuser, M.M. Rajabali, R. Sánchez, N. Smirnova, V. Somà, D.T. Yordanov, Shell structure of potassium isotopes deduced from their magnetic moments, Phys. Rev. C 90 (2014) 034321, https://doi.org/10.1103/PhysRevC.90.034321, https://link.aps.org/doi/10.1103/PhysRevC.90.034321.

[15] A. Gade, R.V.F. Janssens, D. Bazin, R. Broda, B.A. Brown, C.M. Campbell, M.P. Carpenter, J.M. Cook, A.N. Deacon, D.-C. Dinca, B. Fornal, S.J. Freeman, T. Glasmacher, P.G. Hansen, B.P. Kay, P.F. Mantica, W.F. Mueller, J.R. Terry, J.A. Tostevin, S. Zhu, Cross-shell excitation in two-proton knockout: structure of ^{52}Ca, Phys. Rev. C 74 (2006) 021302(R), https://doi.org/10.1103/PhysRevC.74.021302, https://link.aps.org/doi/10.1103/PhysRevC.74.021302.

[16] D. Steppenbeck, S. Takeuchi, N. Aoi, P. Doornenbal, M. Matsushita, H. Wang, H. Baba, N. Fukuda, S. Go, M. Honma, J. Lee, K. Matsui, S. Michimasa, T. Motobayashi, D. Nishimura, T. Otsuka, H. Sakurai, Y. Shiga, P.-A. Söderström, T. Sumikama, H. Suzuki, R. Taniuchi, Y. Utsuno, J.J. Valiente-Dobón, K. Yoneda, Evidence for a new nuclear 'magic number' from the level structure of 54Ca, Nature 502 (2013) 207, https://doi.org/10.1038/nature12522.

[17] J. Bjerregaard, O. Hansen, O. Nathan, R. Stock, R. Chapman, S. Hinds, Proton-hole states in 47, 45K, Phys. Lett. B 24 (11) (1967) 568–570, https://doi.org/10.1016/0370-2693(67)90391-7, http://www.sciencedirect.com/science/article/pii/0370269367903917.

[18] E. Newman, J. Hiebert, The (d, 3He) reaction on the N = 28 nuclei at 34 MeV, Nucl. Phys. A 110 (2) (1968) 366–378, https://doi.org/10.1016/0375-9474(68)90546-0, http://www.sciencedirect.com/science/article/pii/0375947468905460.

[19] F. Touchard, P. Guimbal, S. Büttgenbach, R. Klapisch, M.D.S. Simon, J. Serre, C. Thibault, H. Duong, P. Juncar, S. Liberman, J. Pinard, J. Vialle, Isotope shifts and hyperfine structure of 38–47K by laser spectroscopy, Phys. Lett. B 108 (3) (1982) 169–171, https://doi.org/10.1016/0370-2693(82)91167-4, http://www.sciencedirect.com/science/article/pii/0370269382911674.

[20] T. Otsuka, T. Suzuki, R. Fujimoto, H. Grawe, Y. Akaishi, Evolution of nuclear shells due to the tensor force, Phys. Rev. Lett. 95 (2005) 232502, https://doi.org/10.1103/PhysRevLett.95.232502, https://link.aps.org/doi/10.1103/PhysRevLett.95.232502.

[21] R. Broda, J. Wrzesiński, A. Gadea, N. Mărginean, B. Fornal, L. Corradi, A.M. Stefanini, W. Królas, T. Pawłat, B. Szpak, S. Lunardi, J.J. Valiente-Dobón, D. Mengoni, E. Farnea, M.P. Carpenter, G. De Angelis, F. Della Vedova, E. Fioretto, B. Guiot, R.V.F. Janssens, P.F. Mantica, P. Mason, G. Montagnoli, D.R. Napoli, R. Orlandi, I. Pokrovskiy, G. Pollarolo, E. Sahin, F. Scarlassara, R. Silvestri, S. Szilner, C.A. Ur, M. Trotta, S. Zhu, Proton-hole states in the $n = 30$ neutron-rich isotope ^{49}K, Phys. Rev. C 82 (2010) 034319, https://doi.org/10.1103/PhysRevC.82.034319, https://link.aps.org/doi/10.1103/PhysRevC.82.034319.

[22] O.B. Tarasov, D.S. Ahn, D. Bazin, N. Fukuda, A. Gade, M. Hausmann, N. Inabe, S. Ishikawa, N. Iwasa, K. Kawata, T. Komatsubara, T. Kubo, K. Kusaka, D.J. Morrissey, M. Ohtake, H. Otsu, M. Portillo, T. Sakakibara, H. Sakurai, H. Sato, B.M. Sherrill, Y. Shimizu, A. Stolz, T. Sumikama, H. Suzuki, H. Takeda, M. Thoennessen, H. Ueno, Y. Yanagisawa, K. Yoshida, Discovery of ^{60}Ca and implications for the stability of ^{70}Ca, Phys. Rev. Lett. 121 (2018) 022501, https://doi.org/10.1103/PhysRevLett.121.022501, https://link.aps.org/doi/10.1103/PhysRevLett.121.022501.

[23] K. Kreim, M. Bissell, J. Papuga, K. Blaum, M.D. Rydt, R.G. Ruiz, S. Goriely, H. Heylen, M. Kowalska, R. Neugart, G. Neyens, W. Nörtershäuser, M. Rajabali, R.S. Alarcón, H. Stroke, D. Yordanov, Nuclear charge radii of potassium isotopes beyond n=28, Phys. Lett. B 731 (2014) 97–102, https://doi.org/10.1016/j.physletb.2014.02.012, http://www.sciencedirect.com/science/article/pii/S0370269314001038.

[24] R.F. Garcia Ruiz, M.L. Bissell, K. Blaum, A. Ekström, N. Frömmgen, G. Hagen, M. Hammen, K. Hebeler, J.D. Holt, G.R. Jansen, M. Kowalska, K. Kreim, W. Nazarewicz, R. Neugart, G. Neyens, W. Nörtershäuser, T. Papenbrock, J. Papuga, A. Schwenk, J. Simonis, K.A. Wendt, D.T. Yordanov, Unexpectedly large charge radii of neutron-rich calcium isotopes, Nat. Phys. 12 (2016) 594, https://doi.org/10.1038/nphys3645, article L3.

[25] J. Bonnard, S.M. Lenzi, A.P. Zuker, Neutron skins and halo orbits in the *sd* and *pf* shells, Phys. Rev. Lett. 116 (2016) 212501, https://doi.org/10.1103/PhysRevLett.116.212501, https://link.aps.org/doi/10.1103/PhysRevLett.116.212501.

[26] T. Kubo, D. Kameda, H. Suzuki, N. Fukuda, H. Takeda, Y. Yanagisawa, M. Ohtake, K. Kusaka, K. Yoshida, N. Inabe, T. Ohnishi, A. Yoshida, K. Tanaka, Y. Mizoi, BigRIPS separator and ZeroDegree spectrometer at RIKEN RI beam factory, Prog. Theor. Exp. Phys. 2012 (1) (2012) 03C003, https://doi.org/10.1093/ptep/pts064.

[27] N. Fukuda, T. Kubo, T. Ohnishi, N. Inabe, H. Takeda, D. Kameda, H. Suzuki, Identification and separation of radioactive isotope beams by the BigRIPS separator at the RIKEN RI beam factory, in: XVIth International Conference on ElectroMagnetic Isotope Separators and Techniques Related to Their Applications, December 2–7, 2012 at Matsue, Japan, Nucl. Instrum. Methods Phys. Res., Sect. B, Beam Interact. Mater. Atoms 317 (2013) 323–332, https://doi.org/10.1016/j.nimb.2013.08.048, http://www.sciencedirect.com/science/article/pii/S0168583X13009890.

[28] M. Wang, G. Audi, F.G. Kondev, W. Huang, S. Naimi, X. Xu, The AME2016 atomic mass evaluation (II). Tables, graphs and references, Chin. Phys. C 41 (3) (2017) 030003, https://doi.org/10.1088/1674-1137/41/3/030003.

[29] M. Rosenbusch, P. Ascher, D. Atanasov, C. Barbieri, D. Beck, K. Blaum, C. Borgmann, M. Breitenfeldt, R.B. Cakirli, A. Cipollone, S. George, F. Herfurth, M. Kowalska, S. Kreim, D. Lunney, V. Manea, P. Navrátil, D. Neidherr, L. Schweikhard, V. Somà, J. Stanja, F. Wienholtz, R.N. Wolf, K. Zuber, Probing the $n = 32$ shell closure below the magic proton number $z = 20$: mass measurements of the exotic isotopes ^{52,53}K, Phys. Rev. Lett. 114 (2015) 202501, https://doi.org/10.1103/PhysRevLett.114.202501, https://link.aps.org/doi/10.1103/PhysRevLett.114.202501.

[30] C. Louchart, J. Gheller, P. Chesny, G. Authelet, J. Rousse, A. Obertelli, P. Boutachkov, S. Pietri, F. Ameil, L. Audirac, A. Corsi, Z. Dombradi, J. Gerl, A. Gillibert, W. Korten, C. Mailleret, E. Merchan, C. Nociforo, N. Pietralla, D. Ralet, M. Reese, V. Stepanov, The PRESPEC liquid-hydrogen target for in-beam gamma spectroscopy of exotic nuclei at GSI, Nucl. Instrum. Methods Phys. Res., Sect. A, Accel. Spectrom. Detect. Assoc. Equip. 736 (2014) 81–87, https://doi.org/10.1016/j.nima.2013.10.035, http://www.sciencedirect.com/science/article/pii/S0168900213014150.

[31] T. Kobayashi, N. Chiga, T. Isobe, Y. Kondo, T. Kubo, K. Kusaka, T. Motobayashi, T. Nakamura, J. Ohnishi, H. Okuno, H. Otsu, T. Sako, H. Sato, Y. Shimizu, K. Sekiguchi, K. Takahashi, R. Tanaka, K. Yoneda, Samurai spectrometer for RI beam experiments, Nucl. Instrum. Methods Phys. Res., Sect. B 317 (2013) 294–304, https://doi.org/10.1016/j.nimb.2013.05.089, http://www.sciencedirect.com/science/article/pii/S0168583X13007118.

[32] H.N. Liu, A. Obertelli, P. Doornenbal, C.A. Bertulani, G. Hagen, J.D. Holt, G.R. Jansen, T.D. Morris, A. Schwenk, R. Stroberg, N. Achouri, H. Baba, F. Browne, D. Calvet, F. Château, S. Chen, N. Chiga, A. Corsi, M.L. Cortés, A. Delbart, J.-M. Gheller, A. Giganon, A. Gillibert, C. Hilaire, T. Isobe, T. Kobayashi, Y. Kubota, V. Lapoux, T. Motobayashi, I. Murray, H. Otsu, V. Panin, N. Paul, W. Rodriguez, H. Sakurai, M. Sasano, D. Steppenbeck, L. Stuhl, Y.L. Sun, Y. Togano, T. Uesaka, K. Wimmer, K. Yoneda, O. Aktas, T. Aumann, L.X. Chung, F. Flavigny, S. Franchoo, I. Gašparić, R.-B. Gerst, J. Gibelin, K.I. Hahn, D. Kim, T. Koiwai, Y. Kondo, P. Koseoglou, J. Lee, C. Lehr, B.D. Linh, T. Lokotko, M. MacCormick, K. Moschner, T. Nakamura, S.Y. Park, D. Rossi, E. Sahin, D. Sohler, P.-A. Söderström, S. Takeuchi, H. Törnqvist, V. Vaquero, V. Wagner, S. Wang, V. Werner, X. Xu, H. Yamada, D. Yan, Z. Yang, M. Yasuda, L. Zanetti, How robust is the $n = 34$ subshell closure? first spectroscopy of ^{52}Ar, Phys. Rev. Lett. 122 (2019) 072502, https://doi.org/10.1103/PhysRevLett.122.072502, https://link.aps.org/doi/10.1103/PhysRevLett.122.072502.

[33] A. Obertelli, A. Delbart, S. Anvar, L. Audirac, G. Authelet, H. Baba, B. Bruyneel, D. Calvet, F. Château, A. Corsi, P. Doornenbal, J.M. Gheller, A. Giganon, C. Lahonde-Hamdoun, D. Leboeuf, D. Loiseau, A. Mohamed, J.P. Mols, H. Otsu, C. Péron, A. Peyaud, E.C. Pollacco, G. Prono, J.Y. Rousse, C. Santamaria, T. Uesaka, MINOS: a vertex tracker coupled to a thick liquid-hydrogen target for in-beam spectroscopy of exotic nuclei, Eur. Phys. J. A 50 (1) (2014) 8, https://doi.org/10.1140/epja/i2014-14008-y.

[34] C. Santamaria, A. Obertelli, S. Ota, M. Sasano, E. Takada, L. Audirac, H. Baba, D. Calvet, F. Château, A. Corsi, A. Delbart, P. Doornenbal, A. Giganon, A. Gillib-

ert, Y. Kondo, Y. Kubota, C. Lahonde-Hamdoun, V. Lapoux, D. Leboeuf, C. Lee, H. Liu, M. Matsushita, T. Motobayashi, M. Niikura, M. Kurata-Nishimura, H. Otsu, A. Peyaud, E. Pollacco, G. Prono, H. Tokieda, T. Uesaka, J. Zenihiro, Tracking with the MINOS time projection chamber, Nucl. Instrum. Methods Phys. Res., Sect. A, Accel. Spectrom. Detect. Assoc. Equip. 905 (2018) 138–148, https://doi.org/10.1016/j.nima.2018.07.053, http://www.sciencedirect.com/science/article/pii/S016890021830888X.

[35] S. Takeuchi, T. Motobayashi, Y. Togano, M. Matsushita, N. Aoi, K. Demichi, H. Hasegawa, H. Murakami, Nucl. Instrum. Methods Phys. Res., Sect. A, Accel. Spectrom. Detect. Assoc. Equip. 763 (2014) 596–603, https://doi.org/10.1016/j.nima.2014.06.087, http://www.sciencedirect.com/science/article/pii/S0168900214008419.

[36] S. Agostinelli, J. Allison, K. Amako, J. Apostolakis, H. Araujo, P. Arce, M. Asai, D. Axen, S. Banerjee, G. Barrand, F. Behner, L. Bellagamba, J. Boudreau, L. Broglia, A. Brunengo, H. Burkhardt, S. Chauvie, J. Chuma, R. Chytracek, G. Cooperman, G. Cosmo, P. Degtyarenko, A. Dell'Acqua, G. Depaola, D. Dietrich, R. Enami, A. Feliciello, C. Ferguson, H. Fesefeldt, G. Folger, F. Foppiano, A. Forti, S. Garelli, S. Giani, R. Giannitrapani, D. Gibin, J.G. Cadenas, I. González, G.G. Abril, G. Greeniaus, W. Greiner, V. Grichine, A. Grossheim, S. Guatelli, P. Gumplinger, R. Hamatsu, K. Hashimoto, H. Hasui, A. Heikkinen, A. Howard, V. Ivanchenko, A. Johnson, F. Jones, J. Kallenbach, N. Kanaya, M. Kawabata, Y. Kawabata, M. Kawaguti, S. Kelner, P. Kent, A. Kimura, T. Kodama, R. Kokoulin, M. Kossov, H. Kurashige, E. Lamanna, T. Lampén, V. Lara, V. Lefebure, F. Lei, M. Liendl, W. Lockman, F. Longo, S. Magni, M. Maire, E. Medernach, K. Minamimoto, P.M. de Freitas, Y. Morita, K. Murakami, M. Nagamatu, R. Nartallo, P. Nieminen, T. Nishimura, K. Ohtsubo, M. Okamura, S. O'Neale, Y. Oohata, K. Paech, J. Perl, A. Pfeiffer, M. Pia, F. Ranjard, A. Rybin, S. Sadilov, E.D. Salvo, G. Santin, T. Sasaki, N. Savvas, Y. Sawada, S. Scherer, S. Sei, V. Sirotenko, D. Smith, N. Starkov, H. Stoecker, J. Sulkimo, M. Takahata, S. Tanaka, E. Tcherniaev, E.S. Tehrani, M. Tropeano, P. Truscott, H. Uno, L. Urban, P. Urban, M. Verderi, A. Walkden, W. Wander, H. Weber, J. Wellisch, T. Wenaus, D. Williams, D. Wright, T. Yamada, H. Yoshida, D. Zschiesche, Geant4—a simulation toolkit, Nucl. Instrum. Methods Phys. Res., Sect. A, Accel. Spectrom. Detect. Assoc. Equip. 506 (3) (2003) 250–303, https://doi.org/10.1016/S0168-9002(03)01368-8, http://www.sciencedirect.com/science/article/pii/S0168900203013688.

[37] K. Ogata, K. Yoshida, K. Minomo, Asymmetry of the parallel momentum distribution of (p, pn) reaction residues, Phys. Rev. C 92 (2015) 034616, https://doi.org/10.1103/PhysRevC.92.034616, https://link.aps.org/doi/10.1103/PhysRevC.92.034616.

[38] T. Wakasa, K. Ogata, T. Noro, Proton-induced knockout reactions with polarized and unpolarized beams, Prog. Part. Nucl. Phys. 96 (2017) 32–87, https://doi.org/10.1016/j.ppnp.2017.06.002, http://www.sciencedirect.com/science/article/pii/S0146641017300558.

[39] F. Raimondi, C. Barbieri, Algebraic diagrammatic construction formalism with three-body interactions, Phys. Rev. C 97 (2018) 054308, https://doi.org/10.1103/PhysRevC.97.054308, https://link.aps.org/doi/10.1103/PhysRevC.97.054308.

[40] E. Leistenschneider, M.P. Reiter, S. Ayet San Andrés, B. Kootte, J.D. Holt, P. Navrátil, C. Babcock, C. Barbieri, B.R. Barquest, J. Bergmann, J. Bollig, T. Brunner, E. Dunling, A. Finlay, H. Geissel, L. Graham, F. Greiner, H. Hergert, C. Hornung, C. Jesch, R. Klawitter, Y. Lan, D. Lascar, K.G. Leach, W. Lippert, J.E. McKay, S.F. Paul, A. Schwenk, D. Short, J. Simonis, V. Somà, R. Steinbrügge, S.R. Stroberg, R. Thompson, M.E. Wieser, C. Will, M. Yavor, C. Andreoiu, T. Dickel, I. Dillmann, G. Gwinner, W.R. Plaß, C. Scheidenberger, A.A. Kwiatkowski, J. Dilling, Dawning of the $n = 32$ shell closure seen through precision mass measurements of neutron-rich titanium isotopes, Phys. Rev. Lett. 120 (2018) 062503, https://doi.org/10.1103/PhysRevLett.120.062503, https://link.aps.org/doi/10.1103/PhysRevLett.120.062503.

[41] L. Olivier, S. Franchoo, M. Niikura, Z. Vajta, D. Sohler, P. Doornenbal, A. Obertelli, Y. Tsunoda, T. Otsuka, G. Authelet, H. Baba, D. Calvet, F. Château, A. Corsi, A. Delbart, J.-M. Gheller, A. Gillibert, T. Isobe, V. Lapoux, M. Matsushita, S. Momiyama, T. Motobayashi, H. Otsu, C. Péron, A. Peyaud, E.C. Pollacco, J.-Y. Roussé, H. Sakurai, C. Santamaria, M. Sasano, Y. Shiga, S. Takeuchi, R. Taniuchi, T. Uesaka, H. Wang, K. Yoneda, F. Browne, L.X. Chung, Z. Dombradi, F. Flavigny, F. Giacoppo, A. Gottardo, K. Hadyńska-Klęk, Z. Korkulu, S. Koyama, Y. Kubota, J. Lee, M. Lettmann, C. Louchart, R. Lozeva, K. Matsui, T. Miyazaki, S. Nishimura, K. Ogata, S. Ota, Z. Patel, E. Sahin, C. Shand, P.-A. Söderström, I. Stefan, D. Steppenbeck, T. Sumikama, D. Suzuki, V. Werner, J. Wu, Z. Xu, Persistence of the $z = 28$ shell gap around ^{78}Ni: first spectroscopy of ^{79}Cu, Phys. Rev. Lett. 119 (2017) 192501, https://doi.org/10.1103/PhysRevLett.119.192501, https://link.aps.org/doi/10.1103/PhysRevLett.119.192501.

[42] L. Olivier, S. Franchoo, M. Niikura, Z. Vajta, D. Sohler, P. Doornenbal, A. Obertelli, Y. Tsunoda, T. Otsuka, G. Authelet, H. Baba, D. Calvet, F. Château, A. Corsi, A. Delbart, J.-M. Gheller, A. Gillibert, T. Isobe, V. Lapoux, M. Matsushita, S. Momiyama, T. Motobayashi, H. Otsu, C. Péron, A. Peyaud, E.C. Pollacco, J.-Y. Roussé, H. Sakurai, C. Santamaria, M. Sasano, Y. Shiga, S. Takeuchi, R. Taniuchi, T. Uesaka, H. Wang, K. Yoneda, F. Browne, L.X. Chung, Z. Dombradi, F. Flavigny, F. Giacoppo, A. Gottardo, K. Hadyńska-Klęk, Z. Korkulu, S. Koyama, Y. Kubota, J. Lee, M. Lettmann, C. Louchart, R. Lozeva, K. Matsui, T. Miyazaki, S. Nishimura, K. Ogata, S. Ota, Z. Patel, E. Sahin, C. Shand, P.-A. Söderström, I. Stefan, D. Steppenbeck, T. Sumikama, D. Suzuki, V. Werner, J. Wu, Z. Xu, Erratum: Persistence of the $z = 28$ shell gap around ^{78}Ni: first spectroscopy of ^{79}Cu [Phys. Rev. Lett. 119, 192501 (2017)], Phys. Rev. Lett. 121 (2018) 099902, https://doi.org/10.1103/PhysRevLett.121.099902, https://link.aps.org/doi/10.1103/PhysRevLett.121.099902.

[43] Z. Elekes, A. Kripkó, D. Sohler, K. Sieja, K. Ogata, K. Yoshida, P. Doornenbal, A. Obertelli, G. Authelet, H. Baba, D. Calvet, F. Château, A. Corsi, A. Delbart, J.-M. Gheller, A. Gillibert, T. Isobe, V. Lapoux, M. Matsushita, S. Momiyama, T. Motobayashi, H. Otsu, C. Péron, A. Peyaud, E.C. Pollacco, J.-Y. Roussé, H. Sakurai, C. Santamaria, Y. Shiga, S. Takeuchi, R. Taniuchi, T. Uesaka, H. Wang, K. Yoneda, F. Browne, L.X. Chung, Z. Dombrádi, F. Flavigny, S. Franchoo, F. Giacoppo, A. Gottardo, K. Hadyńska-Klęk, Z. Korkulu, S. Koyama, Y. Kubota, J. Lee, M. Lettmann, C. Louchart, R. Lozeva, K. Matsui, T. Miyazaki, M. Niikura, S. Nishimura, L. Olivier, S. Ota, Z. Patel, E. Sahin, C. Shand, P.-A. Söderström, I. Stefan, D. Steppenbeck, T. Sumikama, D. Suzuki, Z. Vajta, V. Werner, J. Wu, Z. Xu, Nuclear structure of ^{76}Ni from the $(p, 2p)$ reaction, Phys. Rev. C 99 (2019) 014312, https://doi.org/10.1103/PhysRevC.99.014312, https://link.aps.org/doi/10.1103/PhysRevC.99.014312.

[44] K. Bennaceur, J. Dobaczewski, Coordinate-space solution of the Skyrme–Hartree–Fock–Bogolyubov equations within spherical symmetry. The program HFBRAD (v1.00), Comput. Phys. Commun. 168 (2) (2005) 96–122, https://doi.org/10.1016/j.cpc.2005.02.002, http://www.sciencedirect.com/science/article/pii/S0010465505002304.

[45] C. Barbieri, Role of long-range correlations in the quenching of spectroscopic factors, Phys. Rev. Lett. 103 (2009) 202502, https://doi.org/10.1103/PhysRevLett.103.202502, https://link.aps.org/doi/10.1103/PhysRevLett.103.202502.

[46] P.G. Hansen, J.A. Tostevin, Direct reactions with exotic nuclei, Annu. Rev. Nucl. Part. Sci. 53 (1) (2003) 219–261, https://doi.org/10.1146/annurev.nucl.53.041002.110406.

[47] R.E. Kass, A.E. Raftery, Bayes factors, J. Am. Stat. Assoc. 90 (430) (1995) 773–795, https://doi.org/10.2307/2291091, http://www.jstor.org/stable/2291091.

[48] T. Otsuka, T. Suzuki, M. Honma, Y. Utsuno, N. Tsunoda, K. Tsukiyama, M. Hjorth-Jensen, Novel features of nuclear forces and shell evolution in exotic nuclei, Phys. Rev. Lett. 104 (2010) 012501, https://doi.org/10.1103/PhysRevLett.104.012501, https://link.aps.org/doi/10.1103/PhysRevLett.104.012501.

[49] Y. Utsuno, T. Otsuka, Y. Tsunoda, N. Shimizu, M. Honma, T. Togashi, T. Mizusaki, Recent advances in shell evolution with shell-model calculations, ARIS2014, https://journals.jps.jp/doi/pdf/10.7566/JPSCP.6.010007, https://doi.org/10.7566/JPSCP.6.010007, https://journals.jps.jp/doi/abs/10.7566/JPSCP.6.010007.

[50] J. Duflo, A. Zuker, Microscopic mass formulas, Phys. Rev. C 52 (1995) R23–R27, https://doi.org/10.1103/PhysRevC.52.R23, https://link.aps.org/doi/10.1103/PhysRevC.52.R23.

[51] C. Qi, A short explanation of the Duflo-Zuker mass model, arXiv:1407.8218, 2014.

[52] L. Gaudefroy, Shell model study of $n \simeq 28$ neutron-rich nuclei, Phys. Rev. C 81 (2010) 064329, https://doi.org/10.1103/PhysRevC.81.064329, https://link.aps.org/doi/10.1103/PhysRevC.81.064329.

[53] S. Ebata, M. Kimura, Low-lying 2^+ states generated by pn-quadrupole correlation and $n = 28$ shell quenching, Phys. Rev. C 91 (2015) 014309, https://doi.org/10.1103/PhysRevC.91.014309, https://link.aps.org/doi/10.1103/PhysRevC.91.014309.

[54] A. Ekström, G.R. Jansen, K.A. Wendt, G. Hagen, T. Papenbrock, B.D. Carlsson, C. Forssén, M. Hjorth-Jensen, P. Navrátil, W. Nazarewicz, Accurate nuclear radii and binding energies from a chiral interaction, Phys. Rev. C 91 (2015) 051301(R), https://doi.org/10.1103/PhysRevC.91.051301, https://link.aps.org/doi/10.1103/PhysRevC.91.051301.

[55] V. Somà, T. Duguet, C. Barbieri, Ab initio self-consistent Gorkov-Green's function calculations of semimagic nuclei: formalism at second order with a two-nucleon interaction, Phys. Rev. C 84 (2011) 064317, https://doi.org/10.1103/PhysRevC.84.064317, https://link.aps.org/doi/10.1103/PhysRevC.84.064317.

[56] V. Somà, C. Barbieri, T. Duguet, Ab initio self-consistent Gorkov-Green's function calculations of semi-magic nuclei: numerical implementation at second order with a two-nucleon interaction, Phys. Rev. C 89 (2014) 024323, https://doi.org/10.1103/PhysRevC.89.024323, https://link.aps.org/doi/10.1103/PhysRevC.89.024323.

[57] V. Somà, P. Navrátil, F. Raimondi, C. Barbieri, T. Duguet, Novel chiral Hamiltonian and observables in light and medium-mass nuclei, arXiv:1907.09790, 2019.

[58] T. Duguet, V. Somà, S. Lecluse, C. Barbieri, P. Navrátil, Ab initio calculation of the potential bubble nucleus ^{34}Si, Phys. Rev. C 95 (2017) 034319, https://doi.org/10.1103/PhysRevC.95.034319, https://link.aps.org/doi/10.1103/PhysRevC.95.034319.